Notch3 is a major regulator of vascular tone in cerebral and tail resistance arteries

E.J. Belin de Chantemèle[1,2,3], K. Retailleau[1,2,3], F. Pinaud[4], E. Vessières[1,2,3], A Bocquet [1,2,3], A.L. Guihot[1,2,3], B. Lemaire [5,6], V. Domenga[5,6], C. Baufreton[4], L. Loufrani[1,2,3], A. Joutel[5,6,7], D. Henrion[1,2,3,4]

1- INSERM U771, Angers, F-49045, France

2- CNRS UMR 6214, Angers, F-49045, France

3- Université d'Angers, Angers, F-49045, France

4- CHU d'Angers, Angers, F-49045, France

5- INSERM, U740, Paris, F-75010, France

6- Université Paris 7 - Denis Diderot, Faculté de Médecine, Site Lariboisière, Paris, F-75010, France

7- AP-HP, Groupe hospitalier LARIBOISIERE-FERNAND-WIDAL, Groupement hospitalier-universitaire Nord, Laboratoire de Génétique, Paris, F-75010, France

Short title: Notch3 and vascular tone

Word Count: body, including references: body, including references: 4301 figure legends: 275 ; abstract : 200 ; and total number of figures : 5 ; 1 table

Author for correspondence:

Daniel Henrion, Pharm.D., PhD.

INSERM U 771, CNRS UMR 6214,

Faculté de Médecine,

49045 Angers,

FRANCE

Tel : +32 41 73 58 45

Fax : +32 41 73 58 95/96

E-mail : daniel.henrion@univ-angers.fr

1

Abstract

Objective: Notch3, a member of the evolutionary conserved Notch receptor family, is primarily expressed in vascular smooth muscle cells. Genetic studies in human and mice revealed a critical role for Notch3 in the structural integrity of distal resistance arteries by regulating arterial differentiation and postnatal maturation.

Methods and Results: We investigated the role of Notch3 in vascular tone in small resistance vessels (tail and cerebral arteries) and large (carotid) arteries isolated from *Notch3* deficient mice using arteriography. Passive diameter and compliance were unaltered in mutant arteries. Similarly, contractions to phenylephrine, KCl, angiotensin II and thromboxane A2 as well as dilation to acetylcholine or sodium nitroprusside were unaffected. However, *Notch3* deficiency induced a dramatic reduction in pressure-induced myogenic tone associated with a higher flow (shear stress)-mediated dilation in tail and cerebral resistance arteries only. Furthermore, RhoA activity and myosin light chain phosphorylation, measured in pressurized tail arteries, were significantly reduced in *Notch3*KO mice. Additionally, myogenic tone inhibition by the Rho kinase inhibitor Y27632 was attenuated in mutant tail arteries.

Conclusions: Notch3 plays an important role in the control of vascular mechano-transduction, by modulating the RhoA/Rho kinase pathway, with opposite effects on myogenic tone and flow-mediated dilation in the resistance circulation.

Condensed abstract

Notch3 regulates arterial differentiation and postnatal maturation of smooth muscle cells. By using arteries from *Notch3* knockout mice we found that *Notch3* plays an important role in the control of resistance arteries mechano-transduction, by modulating the RhoA/Rho kinase pathway, which is involved in pressure-induced (myogenic) tone.

Key words: resistance arteries, myogenic tone, Notch receptors, flow-mediated dilation, local blood flow regulation.

Introduction

Arteries are specified into different calibers and types of vessels to perform different functions. Schematically, the major arteries of the trunk are elastic arteries of large diameter and low resistance. Elastic conduit arteries absorb the hemodynamic stress of cardiac systole and release this energy in the form of sustained blood pressure during diastole. Conversely, distal arteries are muscular arteries of small diameter and high resistance that are critically involved in local regulation of blood flow. Resistance arteries possess a constant basal tone which is tightly regulated by two mechanical stimuli, ie flow and pressure; basal tone provides the background tone upon which other vasoactive systems may act synergistically [1-3]. Flow produces shear stress and triggers dilation, which depends in part on the production of nitric oxide and vasodilator agents, by the endothelial cells [1, 4, 5]. Mechano-transduction of shear stress involves the extracellular matrix and cell structure proteins [6-8]. Pressure-induced (myogenic) contraction is an inherent property of smooth muscle cells. However the robustness and nature of the response vary significantly with vascular bed and vessel caliber [1, 2]. The cellular structures and signaling pathways involved in the mechano-transduction of pressure into constriction have not been completely elucidated. Signaling mechanisms require calcium entry as well as calcium-sensitization of the contractile apparatus. Several lines of investigation implicate actin polymerization in myogenic tone [9]. Furthermore, the RhoA-Rho kinase signaling pathway is a key regulator of the calcium sensitivity and dynamic remodeling of the actin cytoskeleton [10] and we have recently shown that RhoA activation is essential for the development of myogenic tone [11, 12]

The Notch signaling pathway is an evolutionarily conserved intercellular signaling mechanism that plays a central role during vascular development and physiology in vertebrates [13]. The Notch family receptors comprise 4 highly conserved members in human and rodents (Notch1 to Notch4). Among these, Notch3 is primarily expressed in vascular smooth muscle cells [14], and, recent genetic studies in human and mice have highlighted an important role for this receptor in the development and homeostasis of distal arteries [15]. In human, mutations of *NOTCH3* cause CADASIL, an autosomal dominant vascular dementia. Neurological symptoms arise due to a slowly progressive small-artery-disease, characterized by progressive degeneration of smooth muscle cells of small brain arteries [16]. In the mouse, targeted deletion of the *Notch3* gene does not affect viability nor fertility, but results in structural defects of distal arteries, particularly in the brain and the tail. Specifically, in the

3

absence of *Notch3*, smooth muscle cells of distal arteries exhibit an abnormal shape and cytoskeleton because of an impaired arterial differentiation and postnatal maturation. It is noteworthy that major elastic arteries of the trunk appeared preserved at least at the histological level [17, 18].

In this study we investigated the role of Notch3 in the function of small (resistance) and large (compliance) arteries. We examined the mechanical properties and vascular reactivity to vasoactive agents or mechanical stimuli of arteries from wild-type and *Notch3* null mice. We assessed the tail caudal artery and the middle cerebral artery, as distal resistance vessels, and the common carotid artery, a compliance elastic artery with minimum role in arterial resistance. Consistent with our prior observation that elastic artery did not exhibit structural alteration, we found that the mechanical properties and vascular reactivity of mutant carotid arteries were preserved. Importantly, we found that in the tail caudal and middle cerebral arteries, absence of *Notch3* selectively impaired the response to pressure and flow. Furthermore, RhoA activity and myosin light chain phosphorylation were reduced in pressurized mutant tail arteries, and, myogenic tone inhibition elicited by the Rho kinase inhibitor Y-27632 was significantly attenuated in mutant tail arteries. Together these data support a specific role for Notch3 in the mechano-transduction of pressure and flow in the distal resistance arteries through a RhoA/Rho kinase pathway.

Material and methods (detailed in the online supplement: see www.ahajournals.org)

Notch3-/- mice (KO) and their wild-type littermates (WT) were obtained by crossing *Notch3* heterozygous mice. Adult male mice (n= 25 per group) were anesthetized for blood pressure measurement [19] and then killed by CO_2 inhalation. Common carotid, mesenteric, middle cerebral and tail caudal arteries were collected.

Histology was performed as previously described [17].

Pharmacological study was performed on 2 mm long arterial segments mounted on a wire-myograph [20]. Contraction to Phenylephrine (PE), thromboxane A_2 mimetic (U46619) [21] angiotensin II (AngII) and calcium was tested [22]. Concentration-dependent relaxation in

response to Acetylcholine (ACh) was performed with or without NO synthase blockade (L-NAME), and/or cyclooxygenase blockade (indomethacin) [23].

Pressure (myogenic) and flow-dependent tone was determined in isolated arteries cannulated in a video monitored perfusion system [24].

For Western-blotting arterial segments were dissected and snap-frozen in liquid nitrogen. Samples were analysed for eNOS, p-eNOS, caveolin-1, αV-integrin and β3-integrin, RhoA, P38, pP38, P42, pP42, P44, pP44, FAK, pFAK, MLC and pMLC. Preliminary immunoblot analysis showed that comparable results were obtained using freshly isolated arteries as compared to pressurized (75 mmHg) arterial segments (figure I: see ahajournals.org).

RhoA activation was assessed as previously described [25] using a Rho-GTP pull-down assay kit.

Statistical analysis

Results were expressed as means ± standard error. Significance of the differences between groups was determined by analysis of variance (ANOVA for consecutive measurements for pressure-diameter curves) or one-way ANOVA followed by Bonferroni or paired t-test. P values less than 0.05 were considered to be significant.

Results

Structural and mechanical properties of KO arteries

High-resolution optic microscopy showed structural defects of the mutant caudal artery and middle cerebral artery with thinning and disorganization of the tunica media as previously reported [17]. By contrast, carotid artery of *Notch3* null mice appeared indistinguishable from the one of WT mice (figure II: see ahajournals.org). To determine the effect of absence of *Notch3* on the passive properties of the vascular wall, arteries were submitted to stepwise increase in intraluminal pressure. Passive arterial diameter (figure 1A, Figures VI: see ahajournals.org) and arterial cross sectional compliance (figure 1B and data not shown) were not significantly different in KO and WT mice.

KCl and receptor-dependent contractions

The contraction induced by KCl (80 mmol/L) was not significantly affected by the absence of *Notch3* in carotid, tail caudal and middle cerebral arteries (Figure III and VI: see ahajournals.org). PE, Ang II and U46619 produced a concentration-dependent contraction in carotid and tail caudal arteries. Importantly, contractile responses to these agonists were not significantly different between WT and KO mice (figure 2A, and table 1; figure III and VI: see ahajournals.org). Moreover, the Ca^{2+} dose-response curves in WT and mutant arteries were comparable (figure 2B).

Endothelium-dependent and -independent dilation

Absence of *Notch3* did not significantly affect ACh-induced dilation in carotid, tail, and middle cerebral arteries (figure 2C; Figure IV and VI: see ahajournals.org). Inhibition of NO synthase by L-NAME decreased ACh-induced dilation in carotid and tail caudal arteries with the same potency in WT and KO mice in tail (figure 2C) and carotid arteries (data not shown). Indomethacin did not significantly reduce ACh-induced dilation when added after L-NAME in WT and KO tail (figure 2C) and carotid arteries (data not shown). Endothelium-independent relaxation (SNP) was similar in KO and WT mice (table 1 and data not shown).

Vascular mechano-transduction of flow (shear stress) and pressure

Myogenic tone was significantly decreased by 68 and 75% (measured from the decrease in diameter induced by a pressure of 75 mmHg) in tail and cerebral arteries, respectively, from KO mice compared to WT animals. By contrast, pressure-induced contraction was not significantly different in KO and WT mice in carotid arteries (figure 3, right panel).

Flow mediated dilation (FMD) was significantly higher in mutant tail and cerebral arteries (43% and 30% increase in FMD for a flow rate of 100µl/min) as compared with WT arteries. FMD of WT and mutant carotid arteries were comparable (figure 3, left panel). The precontraction level prior to FMD was similar in WT and KO mice (figure V: see ahajournals.org).

Biochemical analysis

To investigate the mechanisms by which absence of *Notch3* affects mechanotransduction, we assessed the expression level and activation (phosphorylation) of proteins possibly involved in myogenic tone (pP38, P38, pP42, P42, pP44, P44, MLC, pMLC) [2, 9, 11], in FMD (peNOs, eNOs, Cav-1) [1] or in both (FAKs, pFAKs, αV-integrin and β3-integrin) [1, 2] in tail arteries. No

6

difference in protein expression level between WT and mutant mice was found at the exception of pMLC, which was significantly decreased in mutant arteries (figure 4).

In order to further analyze the mechanism involved in the decrease in myogenic tone, we examined the expression level and activity of RhoA. As shown in figure 5 (A-B), *Notch3* null mice exhibited a significant 46% reduction of RhoA activity, while RhoA protein level was unaltered as compared with wild-type mice.

Effect of Rho-kinase inhibition

In order to confirm the involvement of the RhoA/Rho kinase pathway in the mechano-transduction defect observed in *Notch3* null mice, we measured the relaxation induced by stepwise increase in the concentration of the Rho kinase inhibitor Y-27632. Myogenic tone was concentration-dependently inhibited by Y-27632. In control mice, complete inhibition was achieved with 10 μmol/L Y-27632 whereas in *Notch3* deficient mice inhibition reaches only a maximum of 49% at the same dose (figure 5C). We further assessed the relaxation induced by the Rho kinase inhibitor in tail arterial segments preconstricted with KCl (60 mmol/L), PE (0.3 μmol/L), or calcium (0.5 mmol/L). Remarkably, dose-response curves were not significantly different between WT and KO arterial segments (figure 5D,E).

Discussion

Notch3, a key regulator of vascular tone in small arteries

Recently, we demonstrated that Notch3 is critically required for the structural integrity of small distal arteries whereas it appears dispensable for the structural integrity of large conductance arteries [17]. In this study, we provide the first insight into how *Notch3* influences function of the arterial system. Consistent with the notion that Notch3 is dispensable for structural integrity of elastic arteries, we found that the mechanical properties and pharmacological profiles of carotid arteries were unaffected in mice completely lacking *Notch3*. Importantly, we found a significant decrease in myogenic tone and an enhanced flow-mediated dilation in isolated cerebral and tail caudal arteries. These alterations are unlikely to arise from a global dysfunction of vascular cells because both contraction and relaxation to pharmacological agents were unaffected. Hence, the results indicate that *Notch3* deficiency selectively impairs the function of small arteries and suggest a specific role for *Notch3* in the transduction of tensile and shear stress. We reported previously that in the absence of *Notch3*

7

smooth muscle cells of distal arteries lack molecular markers of arterial smooth muscle cells and exhibit histological features of venous cells [17]. Myogenic tone is an inherent property of arterial smooth muscle cells. Thus the present findings indicate that in the absence of *Notch3* smooth muscle cells of distal arteries lack an arterial phenotype also at the functional level and further support the concept that Notch3 is a key regulator of the arterial phenotype of smooth muscle cells.

The ability of small resistance arteries to develop myogenic tone is an important determinant of regional blood flow autoregulation as well as blood pressure [26, 27]. Our prior observation of strongly compromised autoregulation of cerebral blood flow in *Notch3* null mice is consistent with the present finding of an impaired myogenic response in these mice. However, it is remarkable that basal blood pressure is normal in *Notch3* null mice (Supplementary results) [17]. Although activation of cardiac or neurohumoral compensatory mechanisms in *Notch3* null mice might solve this paradox, structural and functional analysis of additional resistance arteries from *Notch3-/-* mice suggests an alternative explanation. Specifically, high-resolution optic microscopy and electron microscopy of mesenteric arteries failed to detect structural defect of smooth muscle cells, although *Notch3* is strongly expressed in these cells (Figure II: see ahajournals.org and data not shown). Moreover, vasoreactivity to pharmacological agents and mechanical stimuli was similar in mutant and wild-type mesenteric arteries (Figure VII: see ahajournals.org). Given the importance of large peripheral vascular beds such as the mesenteric bed in the control of arterial blood pressure a localized vascular change in reactivity is unlikely to cause a significant change in systemic blood pressure. In addition, myogenic tone is mostly involved in the short-term control of local blood flow, whereas hormonal vasoactive systems such as the sympathetic and renin-angiotensin systems have a major role in controlling systemic blood pressure [1, 28]. Thus these later findings suggest that Notch3 is critically required for vascular tone in some vascular beds including at least the brain and the tail arteries, although being dispensable in others including the mesenteric bed.

How does Notch3 influence myogenic tone?

In resistance arteries, increase in intraluminal pressure induces a rapid cell architecture distension leading to the activation of stretch-dependent ion channels and voltage-operated Ca^{2+} channels [29] and ultimately of calmodulin and myosin light chain Kinase [30]. We [11, 12] and others [31-33] have demonstrated the key role played by the RhoA/Rho Kinase pathway in myogenic tone. Moreover, recent studies from our group [12] and others [34] support the

8

hypothesis that activation of integrins and focal-adhesion kinase in caveolin-1 rich domains may participate in the Rho-kinase dependent sensitization of the contractile apparatus to calcium. In the present work, we provide evidence that Notch3 is an upstream modulator of the RhoA/Rho kinase pathway. First, we show that RhoA activity is significantly decreased in the tail arteries lacking *Notch3*. Second, Rho kinase inhibition with Y-27632, in its range of selectivity, was minimally efficient in pressurized mutant tail arteries indicating that the RhoA/Rho kinase activity was reduced in response to pressure (myogenic tone) in the absence of *Notch3*. Third, myosin light chain phosphorylation was significantly reduced in mutant pressurized arteries. The observation that expression levels of integrins, focal adhesion kinase (FAK), ERK1/2 and MAP kinase P38 were not affected by the absence of *Notch3* suggest that Notch3 activity is unrelated or lies downstream to these kinases. The RhoA/Rho kinase pathway has been widely shown to play a key role in the sensitization of the contractile apparatus in response to many vasoconstrictors such as angiotensin II, phenylephrine or thromboxane A2 [10]. However, our data here suggest that only the Rho kinase pathway activated in response to blood pressure elevation is modulated by Notch3. This supports the concept that Notch3 is a key receptor in the signaling pathway translating pressure to contraction (myogenic tone). As previously mentioned, mutant tail arteries exhibit disorganized and disjunctional smooth muscle cells [17]. Using specific inhibitors of gap junction, several studies [31, 35] reported the key role played by cell adhesion in the process of myogenic tone but not agonist-induced vasoconstriction. Assembly of focal adhesion contacts as well as formation of actin filaments bundles (stress fibers) has been reported to be dependent on RhoA activation [36]. Indeed, RhoA participates in the formation of distinct patterns of actin organization and assembly of integrin complexes. It has been reported that, in epithelial cells, RhoA induces the establishment and maintenance of E-Cadherin mediated cell-cell adhesion. Furthermore inactivation of RhoA results in the dislocation of E-cadherin and its complex members from the adherent junction leading to loss of cell-cell adhesion [37]. The reduced RhoA activity observed in the *Notch3* null mice is thus certainly linked to the impaired myogenic tone and to the structural dysfunction observed in vascular smooth muscle cells. Nevertheless further studies are necessary to clarify the exact relationship between Notch3 and RhoA activation.

How does Notch3 activity influence flow-mediated dilation?

In the present study we also demonstrated that *Notch3* null mice exhibited an increased FMD. In endothelial cells, transduction of shear stress into dilation involves integrin-matrix

9

interactions [38] at focal adhesions [39]. FAK activation leads to the phosphorylation of phosphatidylinositol 3-kinase (PI3K) that triggers eNOS activation via the PI3K-Akt pathway [40]. Since Notch3 deficiency did not affect calcium-dependent eNOS activation (ACh), or the effects of eNOS blockade (L-NAME) on ACh-induced dilation, our results rather reflect an increase in shear stress transduction than an enhanced endothelial function.

Several reports show that the pre-existing myogenic tone regulates the vascular response to shear stress [41, 42]. According to the latter authors the higher the intraluminal pressure, the higher is the myogenic tone and the less negative is the resting membrane potential. It would be expected that the open probability time of endothelial potassium channels involved in the FMD would be decreased, while the open probability time of voltage-activated calcium channels associated with constriction in vascular smooth muscle would be increased [29]. We expect the opposite to be true, ie an enhanced FMD in arteries with an attenuated myogenic tone. Nevertheless, the change in myogenic tone could not directly influence the measurement of FMD because of the similar degree of preconstriction applied to arteries from WT and KO mice. It is most likely that the reduced basal tone occurring in vivo influences the sensitivity of the flow-sensing process, although the mechanism involved remains to be determined. Increased FMD in the absence of *Notch3* would thus rather reflect an increased vascular smooth muscle cell capability to dilate in response to shear than an increase endothelium capability to induce dilation. We previously showed that transgenic mice expressing a mutant Notch3 protein, with the R90C mutation (*TgNotchR90C)*, whose expression was specifically targeted in arterial smooth muscle exhibited an increase in myogenic tone associated with a decrease in FMD without endothelial dysfunction [11]. The lack of endothelial dysfunction in these latter mice is one more argument in favor of a regulation of FMD by the pre-existing myogenic tone. At the present time interpretation of the finding that *TgNotchR90C* and *Notch3 KO* mice exhibit opposite vascular dysfunction remains unclear since both *in vitro* and *in vivo* analyses showed that the R90C mutation did not impair canonical Notch3 activity [43, 44].

In summary, the present study provides to the best of our knowledge, the first evidence that Notch3 controls, through the RhoA/ROK signaling pathway, vascular reactivity to the mechanical factors, pressure and flow. Moreover, *Notch3* null mice, because of their highly specific defects, provide an invaluable experimental model to dissect the pathways specifically involved in the modulation of myogenic tone. Finally, our work highlights

Notch3 as a novel pathway for therapeutic targeting in vascular diseases where changes in myogenic responses and vascular autoregulation are thought to play a role.

References:

1.   Henrion D. Pressure and flow-dependent tone in resistance arteries. Role of myogenic tone. *Arch Mal Coeur Vaiss.* 2005;98:913-921.
2.   Hill MA, Davis MJ, Meininger GA, Potocnik SJ, Murphy TV. Arteriolar myogenic signalling mechanisms: Implications for local vascular function. *Clin Hemorheol Microcirc.* 2006;34:67-79.
3.   Dowell FJ, Henrion D, Benessiano J, Poitevin P, Levy B. Chronic infusion of low-dose angiotensin II potentiates the adrenergic response in vivo. *J Hypertens.* 1996;14:177-182.
4.   Vanhoutte PM. Endothelium-derived free radicals: for worse and for better. *J Clin Invest.* 2001;107:23-25.
5.   Qiu HY, Henrion D, Levy BI. Alterations in flow-dependent vasomotor tone in spontaneously hypertensive rats. *Hypertension.* 1994;24:474-479.
6.   Henrion D, Dechaux E, Dowell FJ, Maclour J, Samuel JL, Levy BI, Michel JB. Alteration of flow-induced dilatation in mesenteric resistance arteries of L-NAME treated rats and its partial association with induction of cyclo-oxygenase-2. *Br J Pharmacol.* 1997;121:83-90.
7.   Loufrani L, Matrougui K, Gorny D, Duriez M, Blanc I, Levy BI, Henrion D. Flow (shear stress)-induced endothelium-dependent dilation is altered in mice lacking the gene encoding for dystrophin. *Circulation.* 2001;103:864-870.
8.   Loufrani L, Levy BI, Henrion D. Defect in microvascular adaptation to chronic changes in blood flow in mice lacking the gene encoding for dystrophin. *Circ Res.* 2002;91:1183-1189.
9.   Cipolla MJ, Gokina NI, Osol G. Pressure-induced actin polymerization in vascular smooth muscle as a mechanism underlying myogenic behavior. *Faseb J.* 2002;16:72-76.

10. Loirand G, Guerin P, Pacaud P. Rho kinases in cardiovascular physiology and pathophysiology. *Circ Res.* 2006;98:322-334.

11. Dubroca C, You D, Levy BI, Loufrani L, Henrion D. Involvement of RhoA/Rho kinase pathway in myogenic tone in the rabbit facial vein. *Hypertension.* 2005;45:974-979.

12. Dubroca C, Loyer X, Retailleau K, Loirand G, Pacaud P, Feron O, Balligand JL, Levy BI, Heymes C, Henrion D. RhoA activation and interaction with Caveolin-1 are critical for pressure-induced myogenic tone in rat mesenteric resistance arteries. *Cardiovasc Res.* 2007;73:190-197.

13. Hofmann JJ, Iruela-Arispe ML. Notch signaling in blood vessels: who is talking to whom about what? *Circ Res.* 2007;100:1556-1568.

14. Joutel A, Andreux F, Gaulis S, Domenga V, Cecillon M, Battail N, Piga N, Chapon F, Godfrain C, Tournier-Lasserve E. The ectodomain of the Notch3 receptor accumulates within the cerebrovasculature of CADASIL patients. *J Clin Invest.* 2000;105:597-605.

15. Gridley T. Notch signaling in vascular development and physiology. *Development.* 2007;134:2709-2718.

16. Joutel A, Corpechot C, Ducros A, Vahedi K, Chabriat H, Mouton P, Alamowitch S, Domenga V, Cecillion M, Marechal E, Maciazek J, Vayssiere C, Cruaud C, Cabanis EA, Ruchoux MM, Weissenbach J, Bach JF, Bousser MG, Tournier-Lasserve E. Notch3 mutations in CADASIL, a hereditary adult-onset condition causing stroke and dementia. *Nature.* 1996;383:707-710.

17. Domenga V, Fardoux P, Lacombe P, Monet M, Maciazek J, Krebs LT, Klonjkowski B, Berrou E, Mericskay M, Li Z, Tournier-Lasserve E, Gridley T, Joutel A. Notch3 is required for arterial identity and maturation of vascular smooth muscle cells. *Genes Dev.* 2004;18:2730-2735.

18. Krebs LT, Xue Y, Norton CR, Sundberg JP, Beatus P, Lendahl U, Joutel A, Gridley T. Characterization of Notch3-deficient mice: normal embryonic development and absence of genetic interactions with a Notch1 mutation. *Genesis.* 2003;37:139-143.

19. Baron-Menguy C, Bocquet A, Guihot AL, Chappard D, Amiot MJ, Andriantsitohaina R, Loufrani L, Henrion D. Effects of red wine polyphenols on postischemic neovascularization model in rats: low doses are proangiogenic, high doses anti-angiogenic. *Faseb J.* 2007;21:3511-3521.

20. Loufrani L, Henrion D, Chansel D, Ardaillou R, Levy BI. Functional evidence for an angiotensin IV receptor in rat resistance arteries. *J Pharmacol Exp Ther.* 1999;291:583-588.

21. Bolla M, Matrougui K, Loufrani L, Maclouf J, Levy B, Levy-Toledano S, Habib A, Henrion D. p38 mitogen-activated protein kinase activation is required for thromboxane- induced contraction in perfused and pressurized rat mesenteric resistance arteries. *J Vasc Res.* 2002;39:353-360.

22. Loufrani L, Henrion D. Vasodilator treatment with hydralazine increases blood flow in mdx mice resistance arteries without vascular wall remodelling or endothelium function improvement. *J Hypertens.* 2005;23:1855-1860.

23. Ben Driss A, Devaux C, Henrion D, Duriez M, Thuillez C, Levy BI, Michel JB. Hemodynamic stresses induce endothelial dysfunction and remodeling of pulmonary artery in experimental compensated heart failure. *Circulation.* 2000;101:2764-2770.

24. Dumont O, Loufrani L, Henrion D. Key role of the NO-pathway and matrix metalloprotease-9 in high blood flow-induced remodeling of rat resistance arteries. *Arterioscler Thromb Vasc Biol.* 2007;27:317-324.

25.   Rolli-Derkinderen M, Sauzeau V, Boyer L, Lemichez E, Baron C, Henrion D, Loirand G, Pacaud P. Phosphorylation of serine 188 protects RhoA from ubiquitin/proteasome-mediated degradation in vascular smooth muscle cells. *Circ Res.* 2005;96:1152-1160.

26.   Bevan JA, Laher I. Pressure and flow-dependent vascular tone. *Faseb J.* 1991;5:2267-2273.

27.   Segal SS. Regulation of blood flow in the microcirculation. *Microcirculation.* 2005;12:33-45.

28.   Schubert R, Mulvany MJ. The myogenic response: established facts and attractive hypotheses. *Clin Sci (Lond).* 1999;96:313-326.

29.   Wellman GC, Bevan JA. Barium inhibits the endothelium-dependent component of flow but not acetylcholine-induced relaxation in isolated rabbit cerebral arteries. *J Pharmacol Exp Ther.* 1995;274:47-53.

30.   Davis MJ, Hill MA. Signaling mechanisms underlying the vascular myogenic response. *Physiol Rev.* 1999;79:387-423.

31.   Lagaud G, Gaudreault N, Moore ED, Van Breemen C, Laher I. Pressure-dependent myogenic constriction of cerebral arteries occurs independently of voltage-dependent activation. *Am J Physiol Heart Circ Physiol.* 2002;283:H2187-2195.

32.   Schubert R, Kalentchuk VU, Krien U. Rho kinase inhibition partly weakens myogenic reactivity in rat small arteries by changing calcium sensitivity. *Am J Physiol Heart Circ Physiol.* 2002;283:H2288-2295.

33.   Gokina NI, Park KM, McElroy-Yaggy K, Osol G. Effects of Rho kinase inhibition on cerebral artery myogenic tone and reactivity. *J Appl Physiol.* 2005;98:1940-1948.

34.   Martinez-Lemus LA, Crow T, Davis MJ, Meininger GA. alphavbeta3- and alpha5beta1-integrin blockade inhibits myogenic constriction of skeletal muscle resistance arterioles. *Am J Physiol Heart Circ Physiol.* 2005;289:H322-329.

35.   Earley S, Resta TC, Walker BR. Disruption of smooth muscle gap junctions attenuates myogenic vasoconstriction of mesenteric resistance arteries. *Am J Physiol Heart Circ Physiol.* 2004;287:H2677-2686.

36.   Aspenstrom P, Fransson A, Saras J. Rho GTPases have diverse effects on the organization of the actin filament system. *Biochem J.* 2004;377:327-337.

37.   Takaishi K, Sasaki T, Kotani H, Nishioka H, Takai Y. Regulation of cell-cell adhesion by rac and rho small G proteins in MDCK cells. *J Cell Biol.* 1997;139:1047-1059.

38.   Muller JM, Chilian WM, Davis MJ. Integrin signaling transduces shear stress--dependent vasodilation of coronary arterioles. *Circ Res.* 1997;80:320-326.

39.   Koshida R, Rocic P, Saito S, Kiyooka T, Zhang C, Chilian WM. Role of focal adhesion kinase in flow-induced dilation of coronary arterioles. *Arterioscler Thromb Vasc Biol.* 2005;25:2548-2553.

40.   Dimmeler S, Fleming I, Fisslthaler B, Hermann C, Busse R, Zeiher AM. Activation of nitric oxide synthase in endothelial cells by Akt-dependent phosphorylation. *Nature.* 1999;399:601-605.

41.   Kuo L, Chilian WM, Davis MJ. Interaction of pressure- and flow-induced responses in porcine coronary resistance vessels. *Am J Physiol.* 1991;261:H1706-1715.

42.   Thorin-Trescases N, Bevan JA. High levels of myogenic tone antagonize the dilator response to flow of small rabbit cerebral arteries. *Stroke.* 1998;29:1194-1200; discussion 1200-1191.

43.   Joutel A, Monet M, Domenga V, Riant F, Tournier-Lasserve E. Pathogenic mutations associated with cerebral autosomal dominant arteriopathy with subcortical infarcts and leukoencephalopathy differently affect Jagged1 binding and Notch3 activity via the RBP/JK signaling Pathway. *Am J Hum Genet.* 2004;74:338-347.

44.   Monet M, Domenga V, Lemaire B, Souilhol C, Langa F, Babinet C, Gridley T, Tournier-Lasserve E, Cohen-Tannoudji M, Joutel A. The archetypal R90C CADASIL-NOTCH3 mutation retains NOTCH3 function in vivo. *Hum Mol Genet.* 2007;16:982-992.

Legends to figures

Figure 1:

Passive diameter (A) and cross-sectional compliances (B) of carotid and tail caudal arteries from wild type (WT) and *Notch3*^{-/-} (KO) mice (MEAN ± SEM, n=12 WT and 9 KO); NS, KO versus WT.

Figure 2: Contraction induced by phenylephrine (A) and calcium (B) and vasodilation induced by acetylcholine (C) in the presence of L-NAME (LN) or L-NAME plus indomethacin (LN+INDO) in tail arteries from wild-type (WT) and *Notch3*^{-/-} (KO) mice (MEAN ± SEM, n=12 WT and 9 KO) NS, KO versus WT.

Figure 3: Response of carotid (**A**), tail (**B**) and middle cerebral arteries (**C**) from wild-type (WT) and *Notch3*^{-/-} (KO) to stepwise increase in intraluminal pressure (Myogenic tone, **right panel**) or in intraluminal flow (flow-mediated dilation, **left panel**) (MEAN ± SEM, n=12 WT and 9 KO). *P<0.01, KO versus WT.

Figure 4: Expression level of the MAP kinase P38, P42, P44, FAK, alphaV integrin (αV), beta 3 integrin (β3), myosin light chains (MLC), eNOS and caveolin-1 (cav-1) in tail caudal arteries from wild-type (WT) and *Notch3*^{-/-} (KO) mice. The level of phosphorylated proteins was determined as well (p-P38, p-P42, p-P44, p-FAK, p-MLC and p-eNOS). Shown on the right are representative immunoblots (MEAN ± SEM, n=6 per group). *P<0.05, KO versus WT.

Figure 5: Quantification of RhoA expression level by western-blot (A) and RhoA activity by pull down assay (B) in tail and carotid arteries. The inhibitory effect of the Rho-kinase inhibitor Y27632 (0.01 to 10 µmol/L) was assessed on myogenic tone (C), phenylephrine- (D), KCl (inset in D) as well as on calcium-induced constriction (E) in the tail caudal artery (MEAN ± SEM, n=6 per group). *P<0.01, KO versus WT.

Table 1

Table 1 : Pharmacological profile of *Notch3*-deficient (KO) and wild-type (WT) mice arteries. Contraction to phenylephrine, serotonin (5HT), angiotensin II and U46619 as well as dilation to sodium nitroprusside (SNP) were obtained in tail and carotid arteries.

		Tail artery		Carotid artery		
		WT	KO	WT	KO	units:
Phenylephrine	Emax	7.6 ± 1.0	7.2 ± 0.9	3.2 ± 0.4	3.6 ± 0.4	mN
	EC50	323 ± 78	358 ± 65	45 ± 8	37 ± 7	nmol/L
Angiotensin II	Emax	2.5 ± 0.3	2.4 ± 0.4	1.8 ± 0.3	1.6 ± 0.4	mN
	EC50	3.8 ± 0.7	5.1 ± 0.8	39 ± 6	35 ± 6	nmol/L
U 46619	Emax	6.3 ± 1.0	5.6 ± 0.8	4.8 ± 0.3	5.2 ± 0.5	mN
	EC50	52 ± 11	64 ± 15	79 ± 15	86 ± 17	nmol/L
SNP	Imax	98 ± 2	96 ± 3	98 ± 3	95 ± 4	% dilation
	IC50	32 ± 7	34 ± 6	25 ± 6	19 ± 5	nmol/L

EC_{50} and IC_{50} represent the concentration necessary to reach 50% of the maximal effect; E_{max} and I_{max} give the maximal effect of the drug (n=12 per group).

NS, KO versus WT

A

Carotid artery

Tail artery
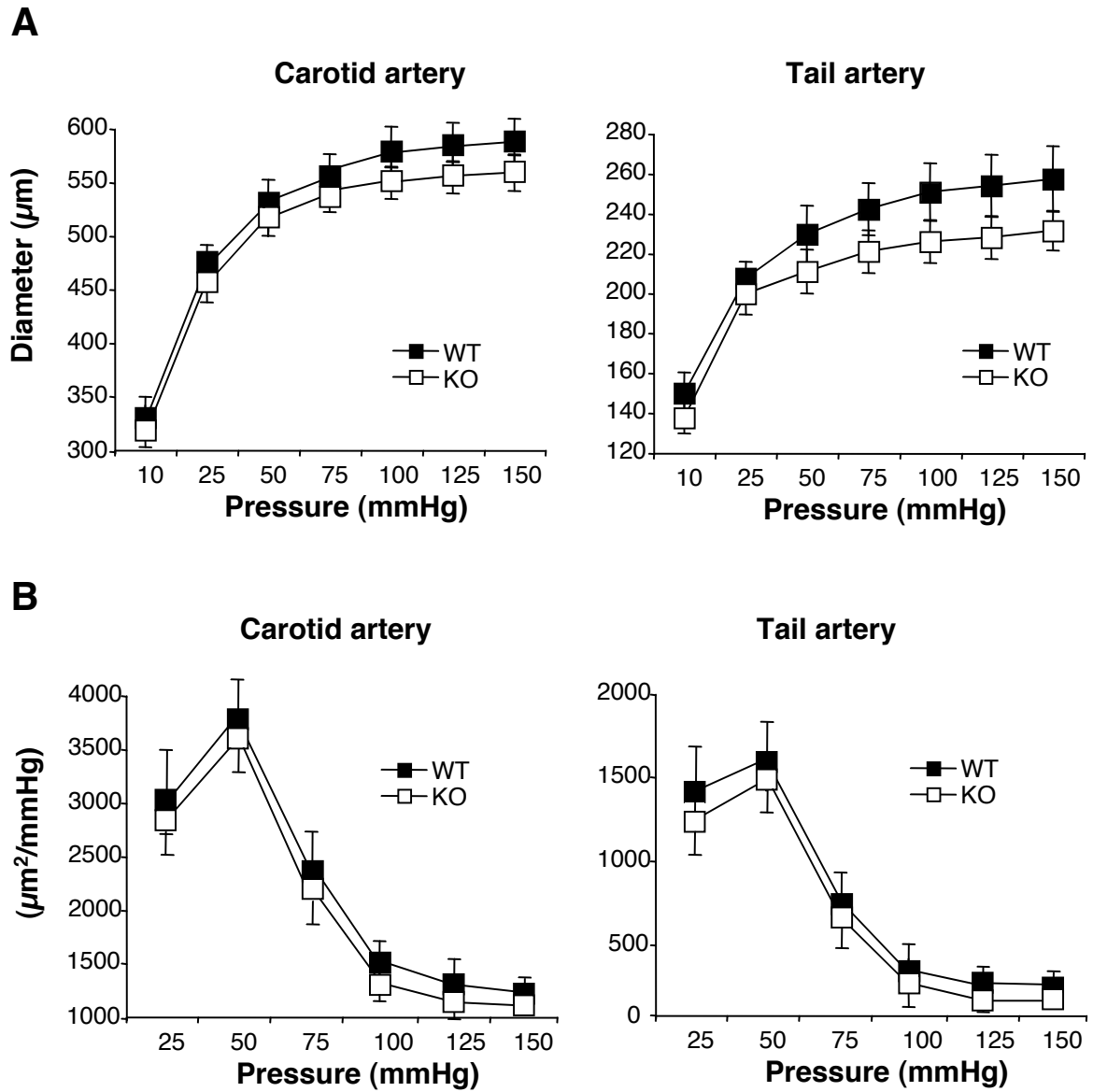

B

Carotid artery

Tail artery

Figure 1: Passive diameter (A) and cross-sectional compliances (B) of carotid and tail caudal arteries from wild type (WT) and *Notch3*^{-/-} (KO) mice (MEAN ± SEM, n=12 WT and 9 KO); NS, KO versus WT.
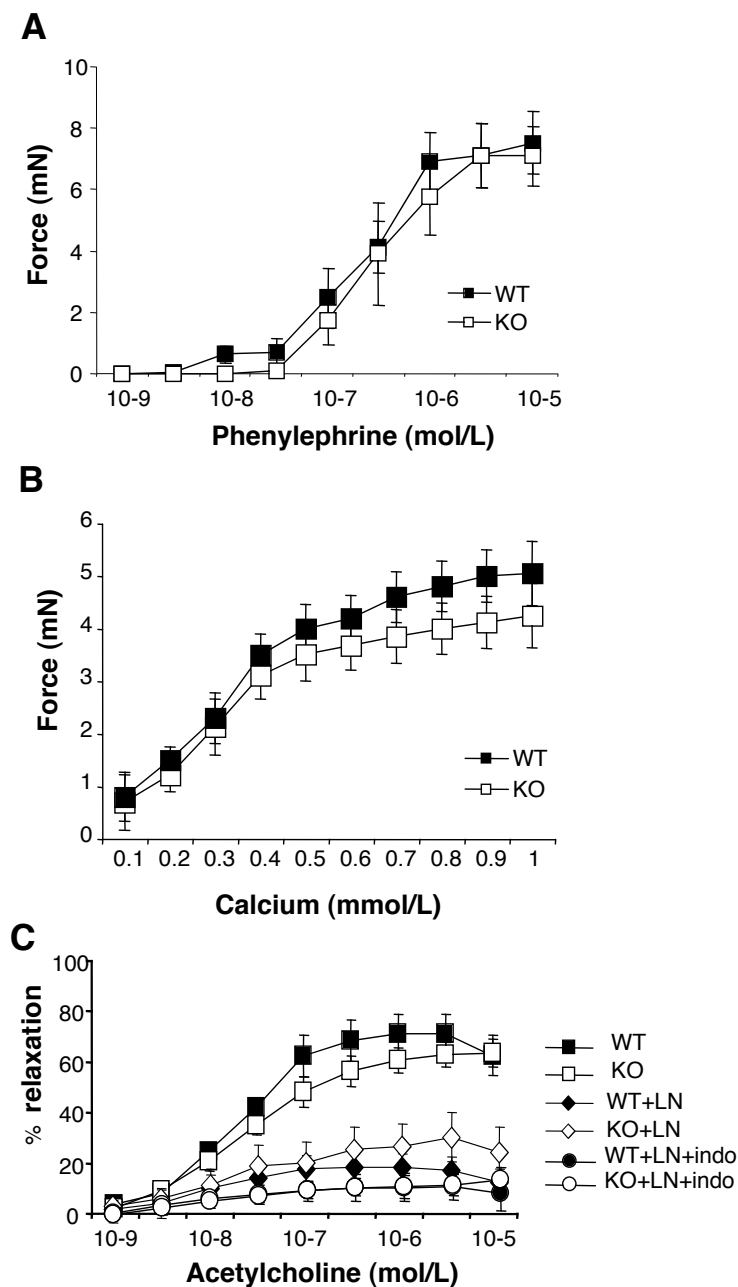
16

Figure 2

A

B

C

Figure 2: Contraction induced by phenylephrine (A) and calcium (B) and vasodilation induced by acetylcholine (C) in the presence of L-NAME (LN) or L-NAME plus indomethacin (LN+INDO) in tail arteries from wild-type (WT) and $Notch3^{-/-}$ (KO) mice (MEAN ± SEM, n=12 WT and 9 KO) NS, KO versus WT.

17

Figure 3

A **Carotid artery**

B **Tail artery**

C **Middle cerebral artery**

Figure 3: Response of carotid (**A**), tail (**B**) and middle cerebral arteries (**C**) from wild-type (WT) and *Notch3*^{-/-} (KO) to stepwise increase in intraluminal pressure (Myogenic tone, **right panel**) or in intraluminal flow (flow-mediated dilation, **left panel**) (MEAN ± SEM, n=12 WT and 9 KO). *P<0.01, KO versus WT.
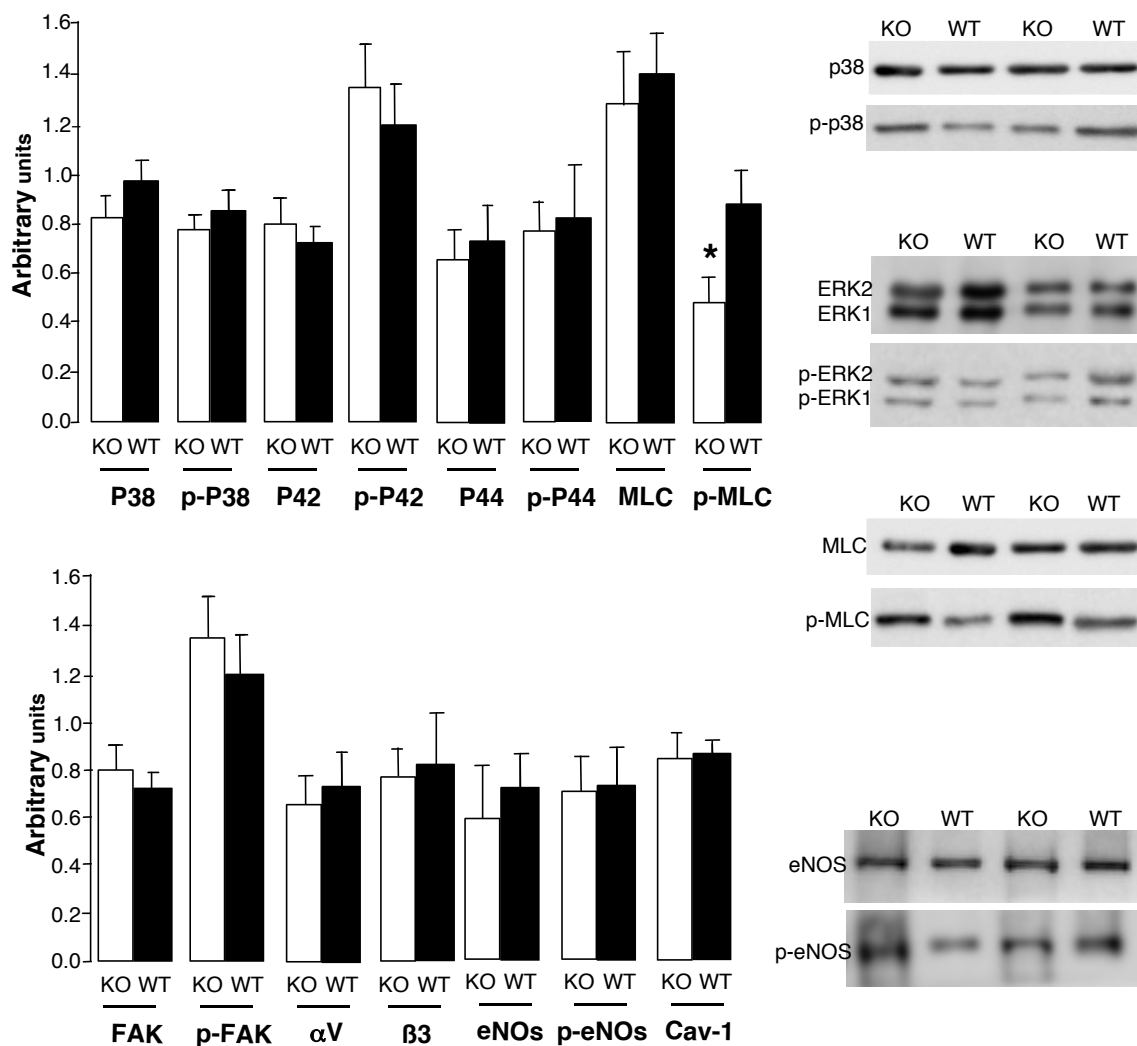
18

Figure 4

Figure 4: Expression level of the MAP kinase P38, P42, P44, FAK, alphaV integrin (αV), beta 3 integrin (β3), myosin light chains (MLC), eNOS and caveolin-1 (cav-1) in tail caudal arteries from wild-type (WT) and *Notch3*^{-/-} (KO) mice. The level of phosphorylated proteins was determined as well (p-P38, p-P42, p-P44, p-FAK, p-MLC and p-eNOS). Shown on the right are representative immunoblots (MEAN ± SEM, n=6 per group). *P<0.05, KO versus WT.
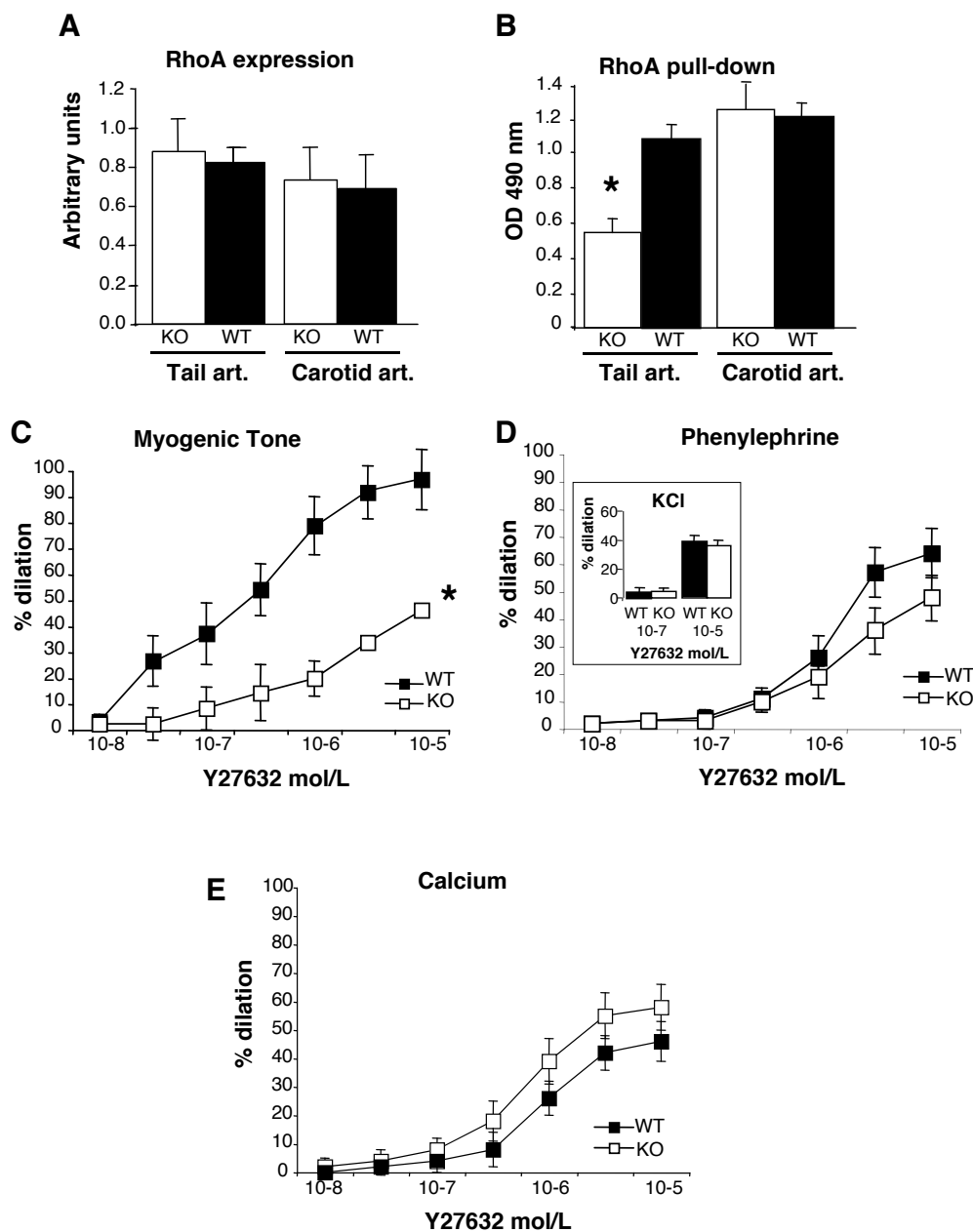
19

Figure 5

A

RhoA expression

B

RhoA pull-down

C **Myogenic Tone**

D **Phenylephrine**

E **Calcium**

Figure 5: Quantification of RhoA expression level by western-blot (A) and RhoA activity by pull down assay (B) in tail and carotid arteries. The inhibitory effect of the Rho-kinase inhibitor Y27632 (0.01 to 10 µmol/L) was assessed on myogenic tone (C), phenylephrine- (D), KCl (inset in D) as well as on calcium-induced constriction (E) in the tail caudal artery (MEAN ± SEM, n=6 per group). *P<0.01, KO versus WT.

SUPPLEMENTS:

Supplementary Material and methods

Animals

The procedure followed in the care and euthanasia of the study animals was in accordance with European Community standards on the Care and Use of Laboratory Animals (Ministère de l'Agriculture, France, authorization no. 6422 and 75-572).

Notch3-/- mice (KO) and their wild-type littermates (WT) were obtained by crossing *Notch3* heterozygous mice. Genomic DNA was obtained from toe biopsy for genotyping by PCR [1]. Adult (10-12 weeks old) male mice (n= 25 WT and 25 KO) were anesthetized using isoflurane (2.5%) and blood pressure measured in the femoral artery [2]. Anesthetized animals were then killed by CO_2 inhalation. Common carotid, mesenteric, middle cerebral and tail caudal arteries were collected for histological, functional and biochemical analysis.

Histological analysis

In order to determine the effects of *Notch3* deletion on vascular structure, carotid, mesenteric, middle cerebral and tail caudal arteries were dissected under a microscope, fixed in CARSON solution and embedded in Epon E812 resin. Semi-thin sections were stained with toluidine blue and observed under a DMR microscope (Leica) as previously described [1].

Pharmacological study in isolated arteries

Arterial segments (2 mm long) were dissected and mounted on a wire-myograph (Danish MyoTechnology, DMT, Aarhus, Denmark), according to the technique of Mulvany and Halpern [3], as previously described [4]. Briefly, 2 tungsten wires (25 μm diameter) were inserted in the lumen of the arteries and fixed to a force transducer and a micrometer, respectively. Arteries were bathed in a 5 ml organ bath containing a physiological salt solution (PSS) maintained at a pH of 7.4, a pO_2 of 160 mmHg and a pCO_2 of 37 mmHg [5]. After wall tension normalization [3], arteries were allowed to stabilize for one hour. Arteries viability was tested using a potassium rich solution (80 mmol/L-PSS). Contractile properties of the artery were tested by Phenylephrine (PE, 0.01 to 10 μmol/L), thromboxane A_2 mimetic (U46619, 10 pmol/L to 0.1 μM) [6] and Angiotensin II (AngII, 1 pmol/L to 0.1 μM) cumulative concentration response curves (CRC). A CRC to calcium (0.1 to 1 mmol/L) was obtained in arteries in a calcium-free PSS [7]. Data were expressed as force developed (mN) in response to the pharmacological stimulation.

In a separate series of experiments, we determined the effect of the Rho-kinase inhibitor Y27632 (0.01 to 10μM) on the contraction induced by PE (0.3 μmol/L), calcium (0.5 mmol/L) or KCl (60 mmol/L) as previously described and data were expressed as percentage of inhibition [8].

Concentration-dependent relaxation in response to Acetylcholine (ACh) (0.01 to 10 μmol/L) was obtained after phenylephrine-serotonin-induced preconstriction (PE 1 μmol/L + 5HT 1 μmol/L). Similar CRC to ACh were realized under NO synthase blockade (L-NAME 100 μmol/L), and NO synthase plus cyclooxygenase blockade (L-NAME 100 μmol/L + indomethacin 10 μmol/L) [9]. Data were expressed as percentage of dilation of phenylephrine-serotonin induced preconstriction [10]. The pharmacological study ended by a dose dependent relaxation curves to sodium nitroprussiate (SNP) (0.01 to 10 μmol/L).

Pressure and flow-dependent tone in isolated arteries

Three-five mm long segment of tail caudal artery (distal part), middle cerebral artery (first segment), mesenteric artery (3^d order) and carotid artery were cannulated at both ends and mounted in a video monitored perfusion system (Living Systems, LSI, Burlington, VT) as previously described [11]. Briefly, cannulated arterial segments were bathed in a 5 ml organ bath containing the PSS described above. Perfusion of the artery was achieved with a similar PSS. Pressure was controlled by a servo-perfusion system and a peristaltic pump-generated flow. Flow-induced dilation was studied by increasing flow rate by steps from 0 to 100 μL.min^{-1}. Data were obtained from arterial segments preconstricted with phenylephrine (PE) at approximately 50-60 % of maximal response and with intraluminal pressure set at 75 mmHg as previously described [12]. Myogenic tone was determined by increasing intraluminal pressure by steps from 10 to 150 mmHg without intraluminal flow. Diameters measured in normal PSS were considered as diameter under active tone or "active diameter". At the end of each experiment arteries were superfused with a Ca^{2+} free PSS containing ethylenbis-(oxyethylenenitrolo) tetra-acetic acid (EGTA, 2 mmol/L), SNP (10 μmol/L) and papaverine (10 μmol/L). Pressure steps were repeated to determine the passive diameter of the arteries. Pressure and diameter measurements were collected by a Biopac® data acquisition system (Biopac MP 100, La Jolla, CA, USA) and continuously recorded. Data were analyzed with the Acqknowledge® software.

In a separate series of experiments, the effect of the Rho-kinase inhibitor Y27632 (0.01 to 10μM) on myogenic tone was determined [8].

Results are given in micrometers for artery diameters. Myogenic tone or active tone was expressed as the percentage of passive diameter ((passive diameter - active diameter) / passive diameter x 100). Flow-induced relaxation was express as percentage dilation of active tone. Arterial cross sectional compliance was calculated using internal diameter values measured under passive conditions (internal passive diameter : PD) over the pressure range of 0-150 mmHg, internal lumen area was calculated as: Ai = pi $\cdot$ PD^2/4 (μm2); cross-sectional compliance (μm2 / mmHg) was then calculated as: Delta Ai/Delta P, in which Delta Ai is the change in internal lumen area induced by a pressure change (Delta P) [5].

Western-blotting

Arterial segments were quickly dissected and snap-frozen in liquid nitrogen. Samples were crushed in liquid nitrogen, resuspended in ice-cold lysis buffer (10 mmol/L Tris-HCl pH 7.4, 1% sodium dodecyl sulfate, 1 mmol/L sodium orthovanadate) and incubated on ice for 30 minutes. The detergent soluble supernatant fractions were collected after centrifugation (14.000 rpm, 20 minutes, 4°C). Protein concentration in samples was equalized using a Micro BCA Protein Assay Kit (Pierce). Proteins (25 μg total protein per sample) were separated by SDS-PAGE (Mini gel protean II system [Bio-Rad], 120 V, with 2.5 mmol/L Tris, 19.2 mmol/L glycine, and 0.01% SDS) using a 4% stacking gel followed by a 12 % running gel. Separated proteins were electrotransferred (120 V, 90 min, 4°C, with 2.5 mmol/L Tris, 19.2 mmol/L glycine, 0.001% SDS and 20% methanol) onto nitrocellulose membranes. Membranes were washed in TBS-T buffer (composed of 20 mmol/L Tris/base pH 7.8, 62 mmol/L NaCl, and 0.1% Tween 20), blocked for 90 minutes at room temperature (10% BSA in TBS-T), incubated over night at 4°C with the primary antibody for eNOS, p-eNOS, caveolin-1, aV-integrin and b3-integrin, RhoA, P38, pP38, P42, pP42, P44, pP44, FAK, pFAK, MLC and pMLC (Transduction Laboratories) followed by incubation with horseradish peroxidase–conjugated antibody (Amersham) 90 minutes at room temperature. Membranes were washed and proteins were visualized using the ECL-Plus Chemiluminescence kit (Amersham). A polyclonal anti-actin antibody (Santa Cruz Biotechnology) was used to

22

reprobe blots to confirm equal loading in lanes. Preliminary immunoblot analysis showed that comparable results were obtained using freshly isolated arteries as compared to pressurized (75 mmHg) arterial segments (figure I, below).

RhoA pull-down assay
RhoA activation was assessed as previously described [13] using a Rho-GTP pull-down assay kit (Cytoskeleton, Denver, USA). Briefly, RhoA activation was determined by affinity precipitation of the active GTP-bound RhoA using a glutathione S-transferase (GST)-fusion protein of the Rho-binding domain of the Rho effector rhotekin (GST-RBD).

References:

1. Domenga V, Fardoux P, Lacombe P, Monet M, Maciazek J, Krebs LT, Klonjkowski B, Berrou E, Mericskay M, Li Z, Tournier-Lasserve E, Gridley T, Joutel A. Notch3 is required for arterial identity and maturation of vascular smooth muscle cells. *Genes Dev.* 2004;18:2730-2735.
2. Baron-Menguy C, Bocquet A, Guihot AL, Chappard D, Amiot MJ, Andriantsitohaina R, Loufrani L, Henrion D. Effects of red wine polyphenols on postischemic neovascularization model in rats: low doses are proangiogenic, high doses anti-angiogenic. *Faseb J.* 2007;21:3511-3521.
3. Mulvany MJ, Halpern W. Contractile properties of small arterial resistance vessels in spontaneously hypertensive and normotensive rats. *Circ Res.* 1977;41:19-26.
4. Loufrani L, Henrion D, Chansel D, Ardaillou R, Levy BI. Functional evidence for an angiotensin IV receptor in rat resistance arteries. *J Pharmacol Exp Ther.* 1999;291:583-588.
5. Loufrani L, Matrougui K, Gorny D, Duriez M, Blanc I, Levy BI, Henrion D. Flow (shear stress)-induced endothelium-dependent dilation is altered in mice lacking the gene encoding for dystrophin. *Circulation.* 2001;103:864-870.
6. Bolla M, Matrougui K, Loufrani L, Maclouf J, Levy B, Levy-Toledano S, Habib A, Henrion D. p38 mitogen-activated protein kinase activation is required for thromboxane- induced contraction in perfused and pressurized rat mesenteric resistance arteries. *J Vasc Res.* 2002;39:353-360.
7. Loufrani L, Henrion D. Vasodilator treatment with hydralazine increases blood flow in mdx mice resistance arteries without vascular wall remodelling or endothelium function improvement. *J Hypertens.* 2005;23:1855-1860.
8. Dubroca C, You D, Levy BI, Loufrani L, Henrion D. Involvement of RhoA/Rho kinase pathway in myogenic tone in the rabbit facial vein. *Hypertension.* 2005;45:974-979.
9. Ben Driss A, Devaux C, Henrion D, Duriez M, Thuillez C, Levy BI, Michel JB. Hemodynamic stresses induce endothelial dysfunction and remodeling of pulmonary artery in experimental compensated heart failure. *Circulation.* 2000;101:2764-2770.
10. Loufrani L, Matrougui K, Li Z, Levy BI, Lacolley P, Paulin D, Henrion D. Selective microvascular dysfunction in mice lacking the gene encoding for desmin. *Faseb J.* 2002;16:117-119.
11. Dumont O, Loufrani L, Henrion D. Key role of the NO-pathway and matrix metalloprotease-9 in high blood flow-induced remodeling of rat resistance arteries. *Arterioscler Thromb Vasc Biol.* 2007;27:317-324.
12. Henrion D, Dechaux E, Dowell FJ, Maclour J, Samuel JL, Levy BI, Michel JB. Alteration of flow-induced dilatation in mesenteric resistance arteries of L-NAME

treated rats and its partial association with induction of cyclo-oxygenase-2. *Br J Pharmacol.* 1997;121:83-90.

13. Rolli-Derkinderen M, Sauzeau V, Boyer L, Lemichez E, Baron C, Henrion D, Loirand G, Pacaud P. Phosphorylation of serine 188 protects RhoA from ubiquitin/proteasome-mediated degradation in vascular smooth muscle cells. *Circ Res.* 2005;96:1152-1160.

Supplementary results

Animals

Body weights of *Notch3-/-* mice (25±1.6g, n= 10) were comparable to those of wild-type littermate mice (26±1.4g, n=10). Blood pressure was measured in the femoral artery. Mean blood pressure did not differ between Notch3 null mice (88±2 mmHg, n=10) and wild-type mice (92±3mmHg, n=10).

Supplementary Figures

Figure I: pMLC/MLC level is identical in freshly isolated tail arteries and in pressurized arterial segments
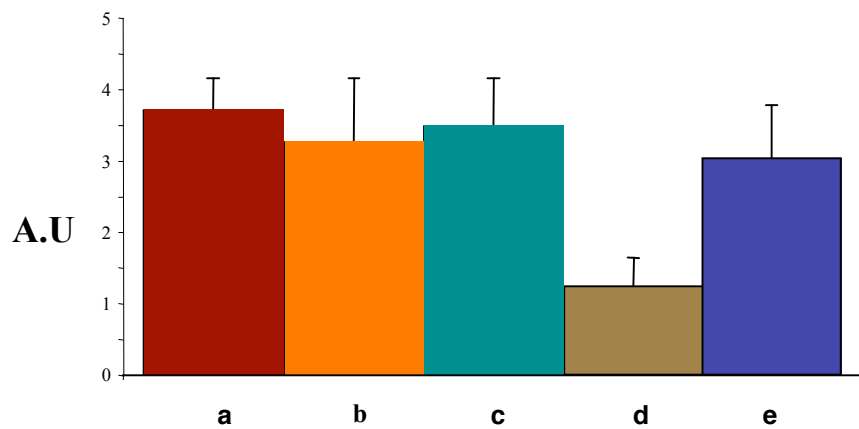
To test the hypothesis that activation of proteins, which are involved in myogenic tone, remains intact in quickly dissected arteries, we compared level of p-MLC in pressurized arterial segments and in freshly isolated arteries. The p-MLC/MLC ratio was determined by immunoblot analysis of tail caudal arteries processed as indicated: (a) arteries were freshly and quickly dissected and snap-frozen in liquid nitrogen, (b) arteries were freshly and quickly dissected and snap-frozen in liquid nitrogen after a one hour incubation in PSS at 4°C, (c) arterial segments were dissected in PSS at 4°C, mounted in an arteriograph + 60 min under a pressure of 75 mmHg (37°C) and then snap-frozen. As positive and negative controls, arteries were incubated 30 min in PSS at room temperature before being frozen (d) or stimulated with phenylephrine (1µm/L) 30 min in PSS at room temperature (e).

(n=4 tail arteries per group in a,b, d and e and n= 3 samples of 10 pooled arterial segments in c). A.U.= arbitrary unit.

Figure II: Structural properties of arteries from *Notch3* null mice
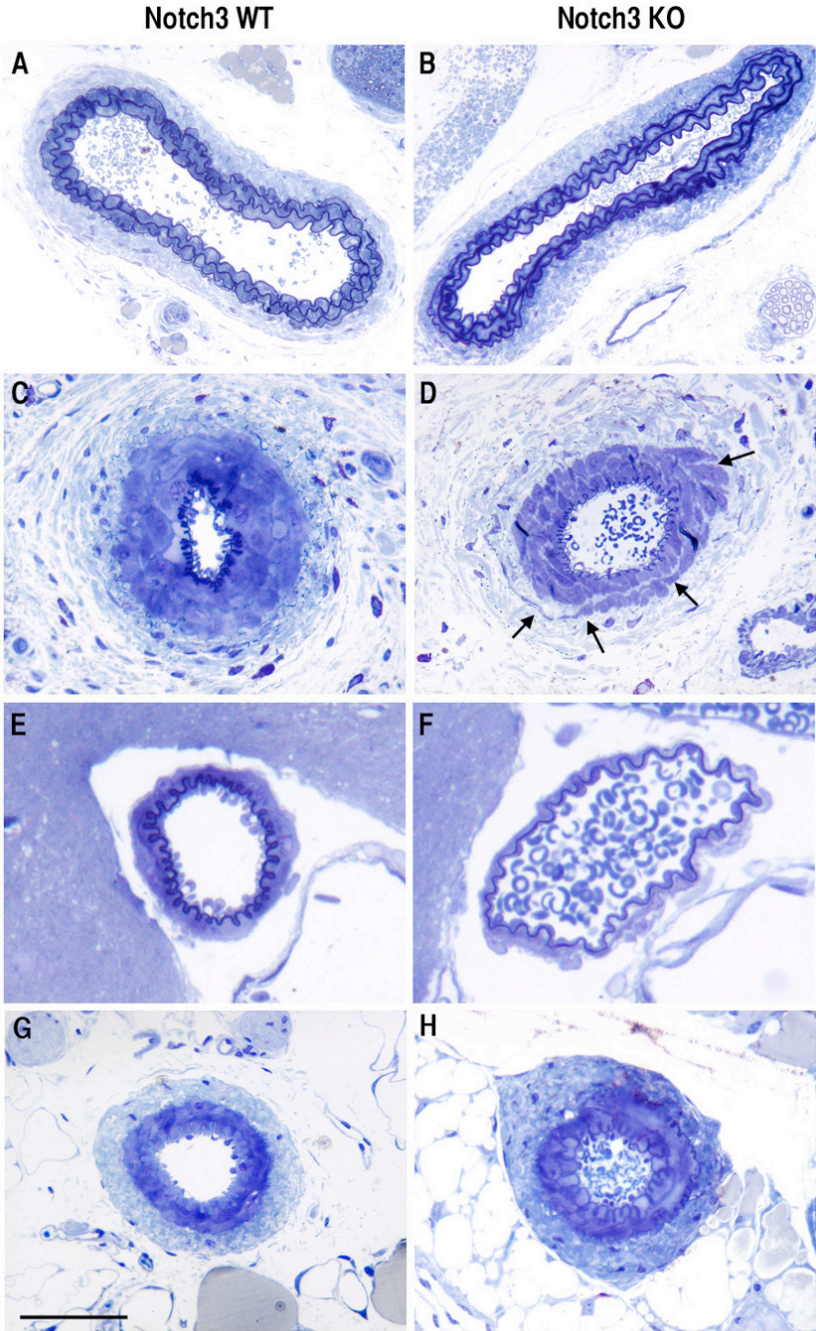

Semi-thin sections of arteries from wildtype and *Notch3 KO* mice were stained by toluidine blue. Shown are representative sections of carotid arteries (A-B), caudal tail arteries (C-D), middle cerebral arteries (E-F) and mesenteric arteries (G-H). Note the thinner media in the mutant tail and cerebral arteries with thinner smooth muscle cells, as well as the non cohesive smooth muscle cells in the media of the caudal artery (arrows) while mutant carotid and mesenteric arteries exhibit no obvious defect. Scale bar : 120µm (A,B) and 60µm (C-H)

Figure III: KCl and receptor-dependent contractions in tail and carotid arteries

A

KCl-induced contraction

B

Angiotensin II (mol/L)

C

U46619 (mol/L)
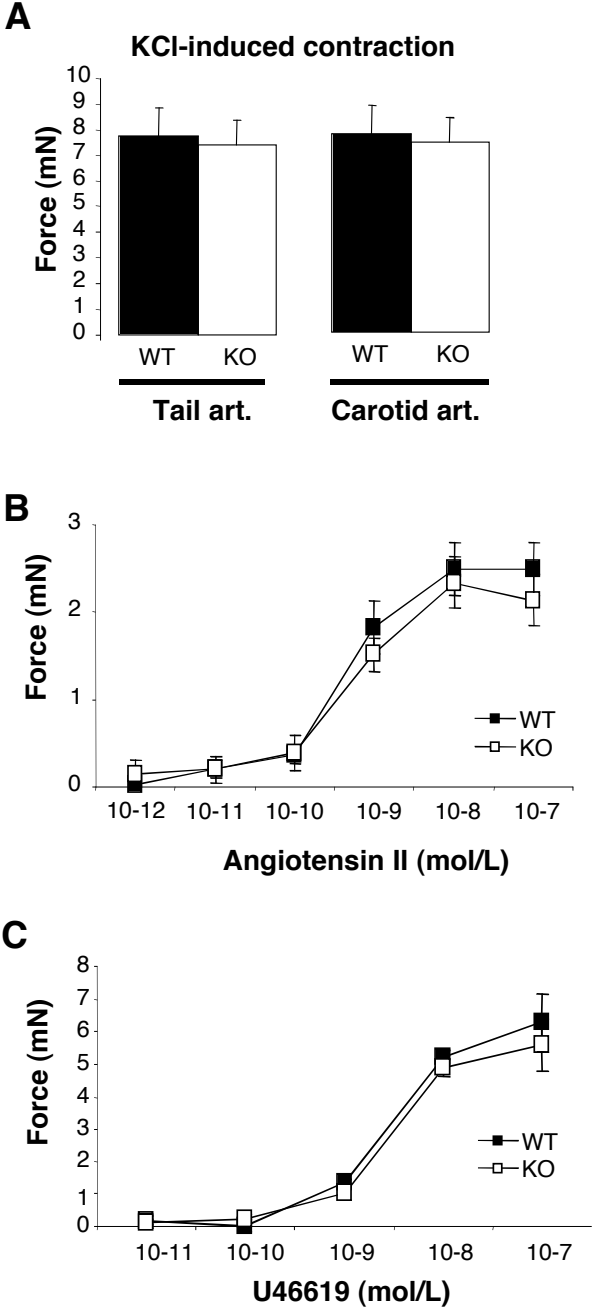
Vasoconstriction induced by KCl (80 mmol/L, **A**), angiotensin II (**B**) and the thromboxane A2 analog U46619 (**C**) was investigated in tail (A-C) and carotid arteries (art.) (A) isolated from *Notch3* KO mice and their wild-type (WT) control (n=12 WT and 9 KO). NS, KO versus WT.
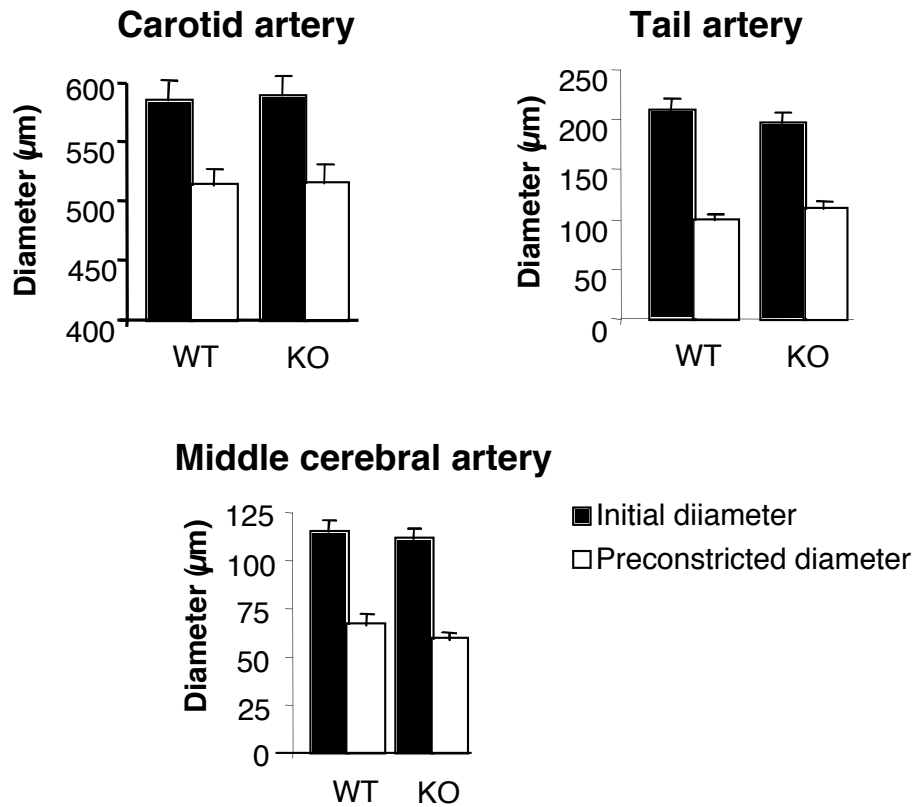
Figure IV: Acetylcholine-induced dilation in tail and carotid arteries

A

B
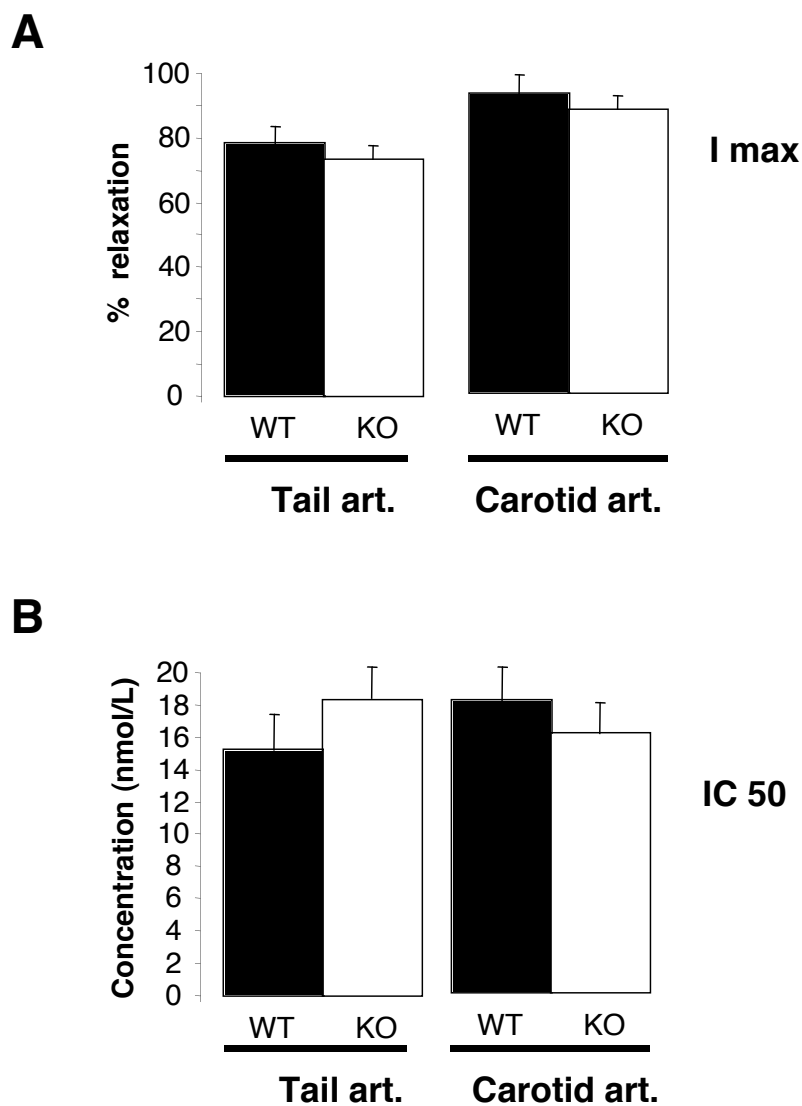
Cumulative concentration response curve to Acetylcholine performed in tail and carotid arteries from wild-type (WT) and *Notch3*$^{-/-}$ (KO) mice. Imax (**A**) and IC50 (**B**) calculated from cumulative concentration response curves.
Data are presented as MEAN ± SEM. (n=12 WT and 9 KO). NS, KO versus WT.

Figure V: Preconstriction induced prior to flow-mediated dilation

Carotid artery

Tail artery

Middle cerebral artery

■ Initial diiameter
□ Preconstricted diameter

Preconstriction in carotid, tail and middle cerebral arteries isolated from wild-type (WT) and *Notch3*$^{-/-}$ (KO) mice, induced prior to flow-mediated dilation (data in figure 3), are presented. NS, KO versus WT.
Data are presented as MEAN ± SEM. (n=12 WT and 9 KO).

Figure VI: Mechanical properties and vasoreactivity of middle cerebral arteries

A
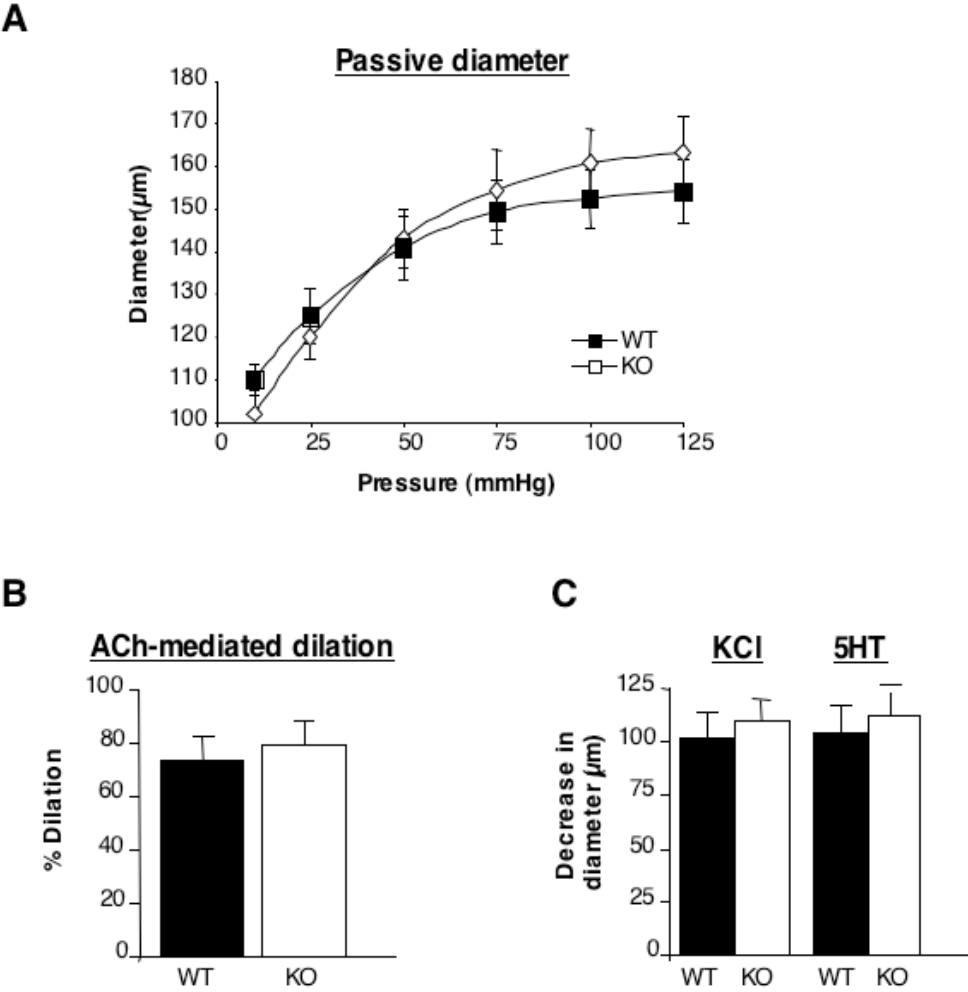
A: Changes in passive diameter in response to stepwise increases in pressure
B: Vasodilation induced by acetylcholine (ACh, 1μmol/L)
C: Vasoconstriction induced by KCl (80 mmol/L) and by serotonin (5HT, 1 μmol/L).
Middle cerebral arteries were isolated from wild-type (WT) and *Notch3*^{-/-} (KO) mice. Data are presented as MEAN ± SEM. (n=5 WT and 5 KO). NS, KO versus WT.

Figure VII: Mechanical properties and vasoreactivity of mesenteric arteries are unaltered in *Notch3* KO mice
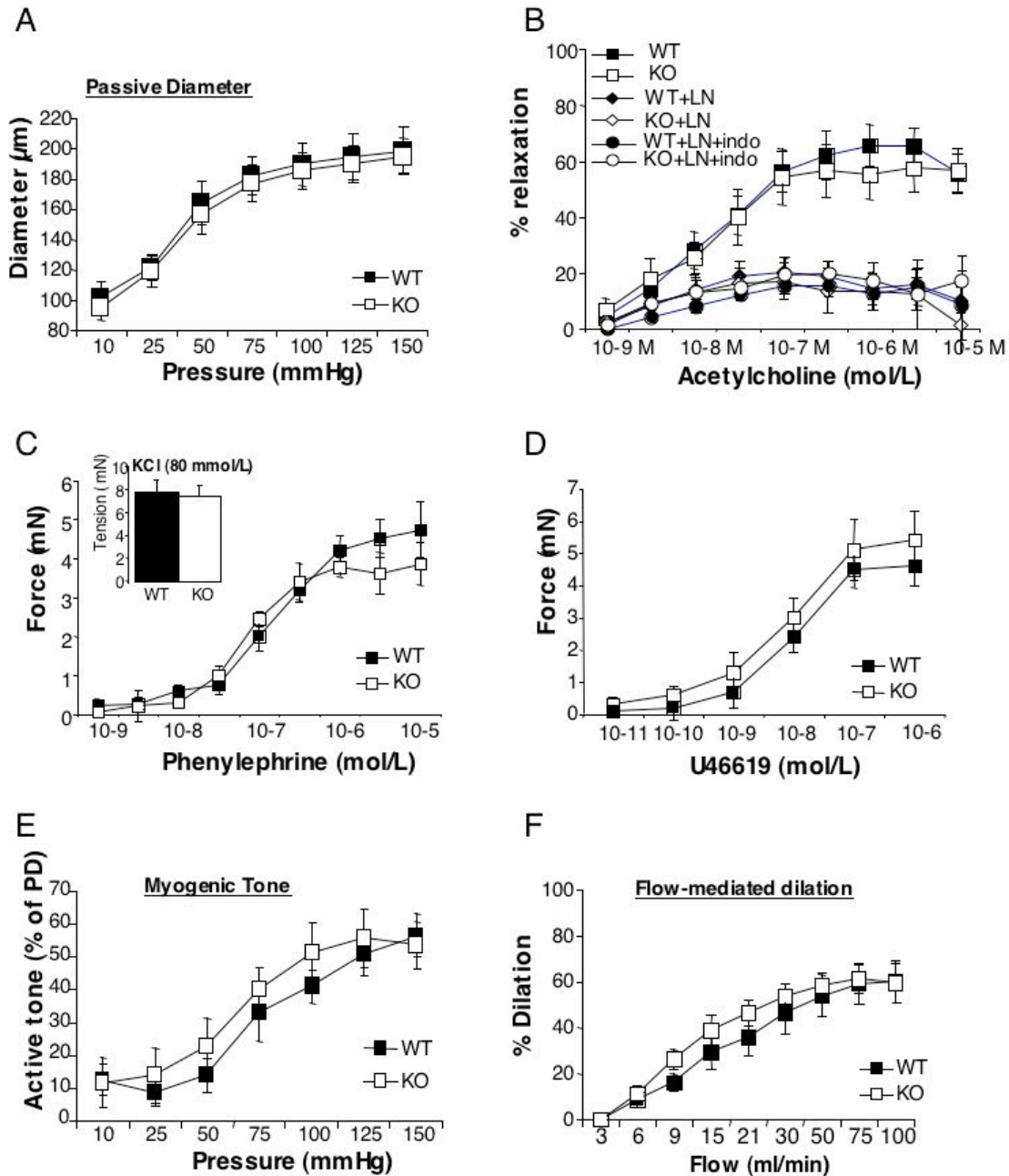
A: Changes in passive diameter in response to stepwise increases in pressure
B: Cumulative concentration response curve to Acetylcholine performed in the presence of the NO-synthase inhibitor L-NAME (LN) or L-NAME plus the cycloxygenase inhibitor indomethacine (LN+INDO).
C: Constriction induced by a potassium-rich (KCl, 80 mmol/L) and phenylephrine.
D: Constriction induced by the thromboxane A_2 mimetic U46619
E: Response to stepwise increases in intraluminal pressure (Myogenic tone).
F: Response to stepwise increases in intraluminal blood flow (Flow-mediated dilation) .
Mesenteric resistance arteries were isolated from wild-type (WT) and *Notch3*^{-/-} (KO) mice.
Data are presented as MEAN ± SEM. (n=12 WT and 9 KO). NS, KO versus WT